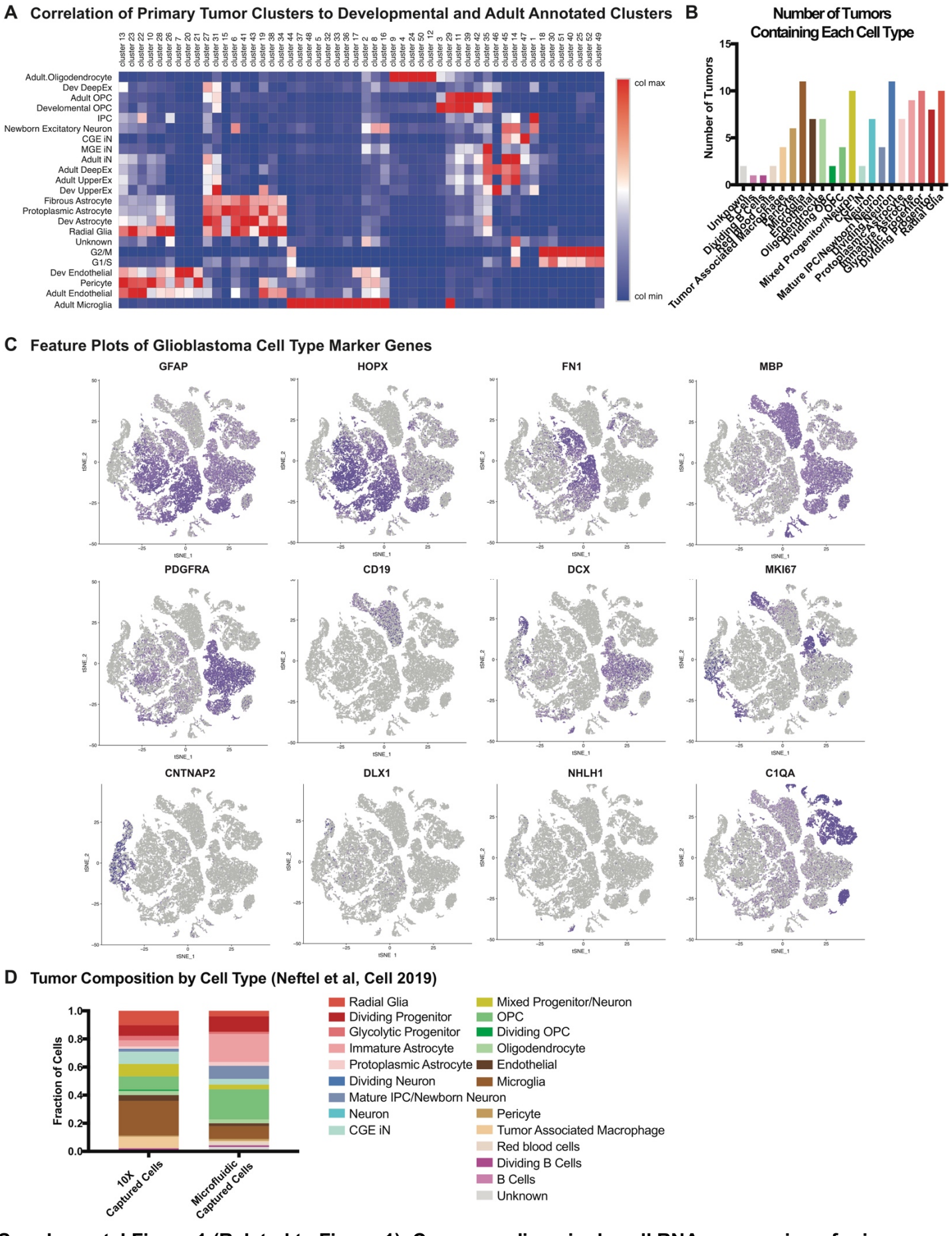

Supplemental Figure 1 (Related to Figure 1). Corresponding single cell RNA-sequencing of primary

glioblastoma tumors to known cell types a) Correlation matrix of each primary glioblastoma to annotated cell types from adult cortex and development. For each row, the column (col) min to the column max is shown as a gradient from blue to red. The reddest box for each column represents the cell type which most resembles the glioblastoma cluster. **b)** Graph shows the number of tumors in which each cell type has been identified of the 11 tumors sequenced in this study. **c)** Feature plots of marker genes (also shown as violin plots in Fig 1C) with gray representing no expression and dark purple representing maximal expression. **d)** Stacked barplot of cell type composition for cells analyzed from Neftel et al 2019, indicating the presence of cell type heterogeneity, including outer radial glia cells.

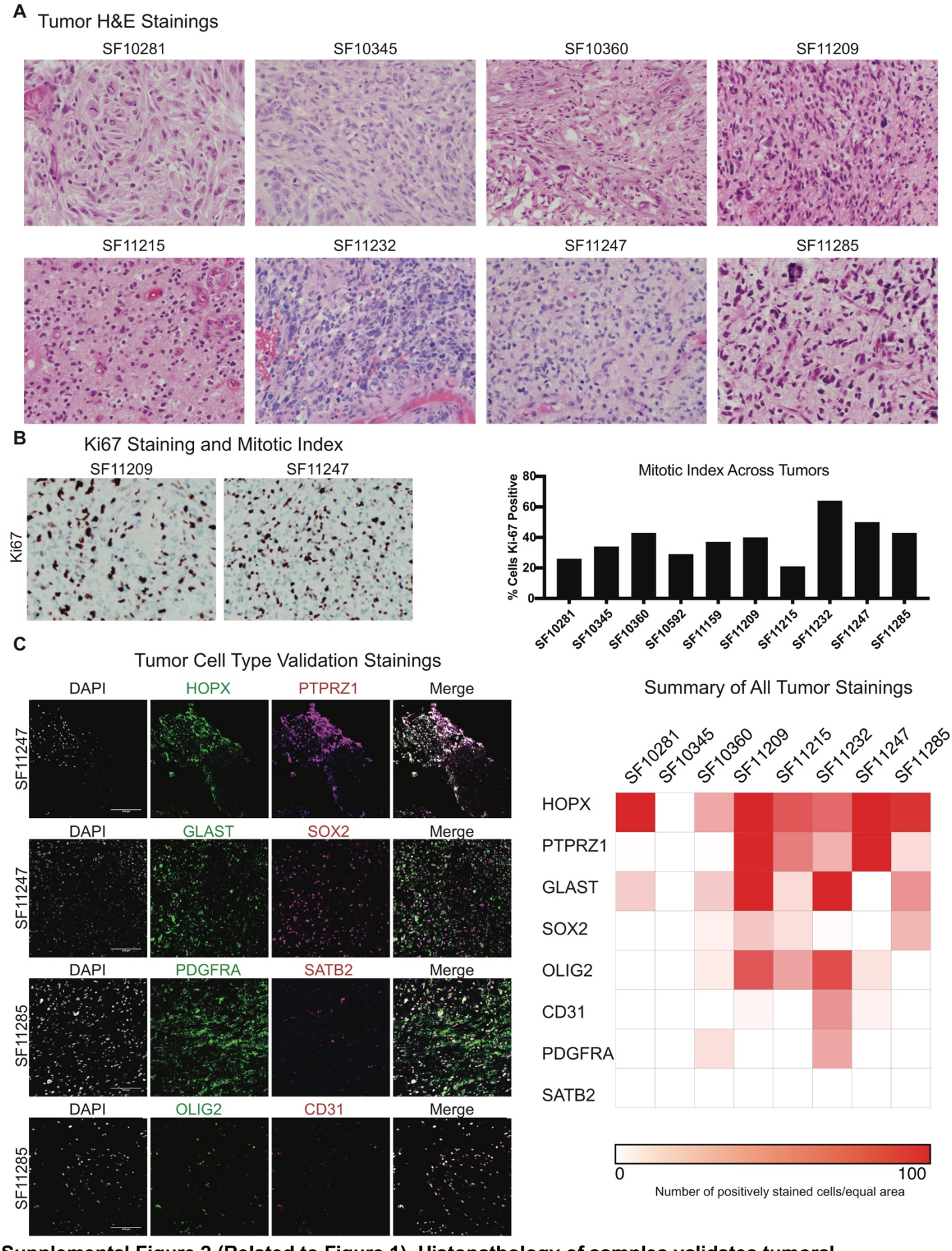

Supplemental Figure 2 (Related to Figure 1). Histopathology of samples validates tumoral

heterogeneity and a subset of cell type composition a) Tumor hematoxylin and eosin stain of 8 of the tumors sampled in this study. Varied tumor structure and differentiation status is observed, consistent with prior reports of tumor heterogeneity. **b)** Two representative Ki67 stainings are shown that were used to label dividing cells and calculate a mitotic index. Tumors vary in their Ki67 staining (show in bar chart), but all GBM samples consistently have above 20% of cells in mitosis. **c)** Immunofluorescent stains were performed on banked samples corresponding to the tumors that were analyzed. The markers chosen corresponded to markers of major cell populations identified from the MetaCluster analysis. The heatmap on the right summarizes the degree of validation observed in the 8 tumors that were validated, as quantified by the number of positively stained cells within an equal area of tumor. Each tumor expresses at least one of the observed cell types and many have representation from multiple clusters. Scale bar = 100 μM.

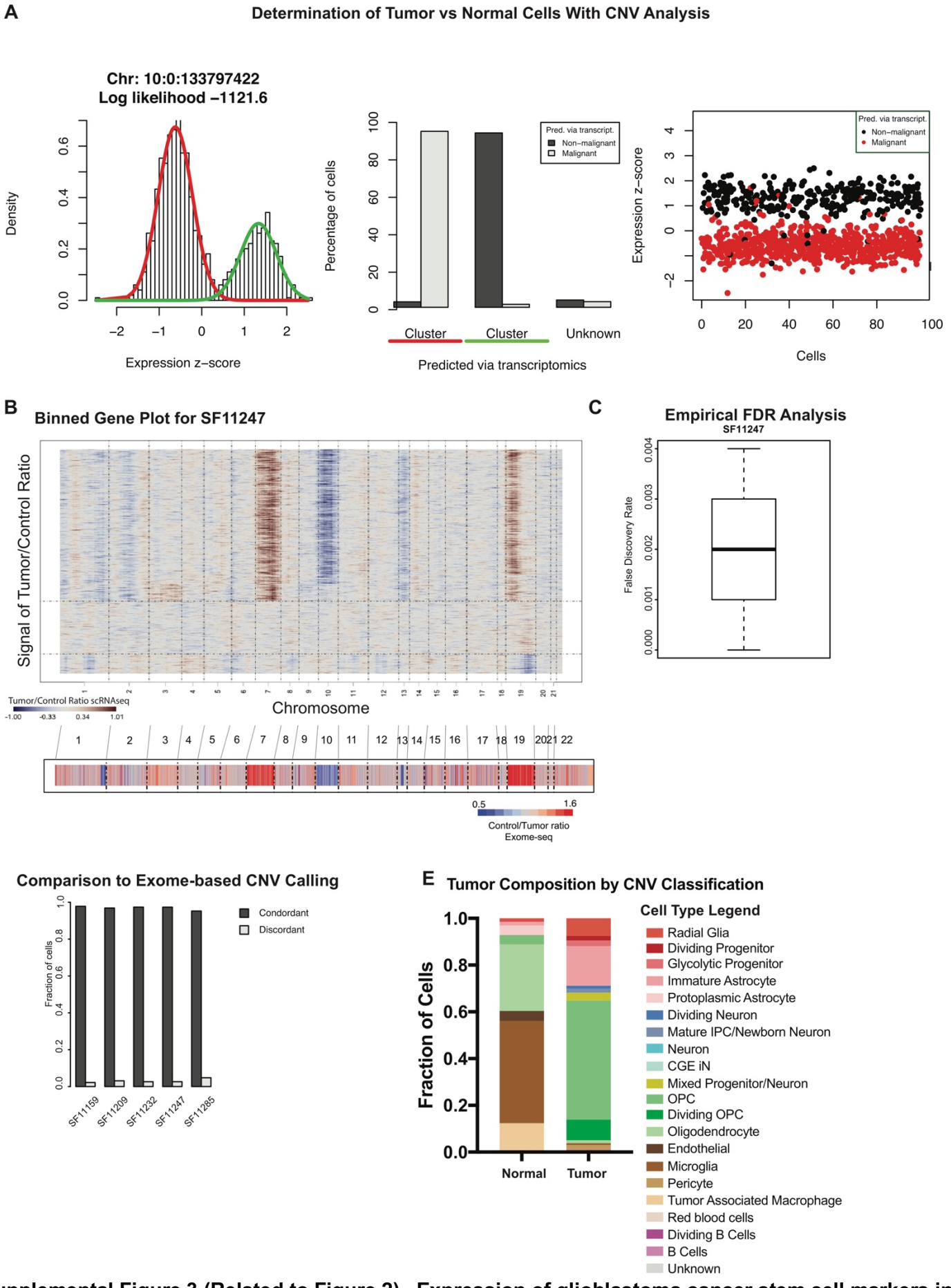

Supplemental Figure 3 (Related to Figure 2). Expression of glioblastoma cancer stem cell markers in a

variety of cell types including IVY database a) Additional feature plots of cancer stem cell markers in single-cell RNA sequencing shows both broad and very sparse expression of genes associated with cancer stemness identity. **b)** Representative images of immunohistochemistry of a number of markers from the IVY database show both glioblastoma cancer stem cell markers and cell type identification markers can be broadly expressed throughout the tumor, and often co-localize. The cancer stem cell markers are not frequently restricted to a single cell type, as shown by the co-localization of progenitor (HES6) and interneuron (DLX5) expression with the expression of cancer stem cell markers. **c)** Heatmap depicting data from IVY Glioblastoma database recapitulates observations in single-cell analysis, with each tumor expressing a heterogeneity of cancer stem cell markers and cell type markers as indicated by the red signal in the heatmap. Genes marked by light blue at the top key across columns indicates normal genes that are used as cell type markers, while the darker blue and green represent Tier 1 and Tier 2 glioblastoma cancer stem cell (GSC) genes respectively. The Tier 1 genes are the most validated GSC genes and Tier 2 are hypothesized to play an important role in GSC biology. The heatmap depicts that within each tumor in each row, expression of a variety of cell identity genes can be co-expressed with many GSC genes. **d)** Scatterplots depict the expression of a glioblastoma cancer stem cell marker (x – axis) and the expression of cell type identifier markers (as defined by the normal genes in the above heatmap) (y – axis) as generated from expression data in the IVY Glioblastoma database. Each dot represents a co-expression pattern in a single tumor of a cell type marker with a cancer stem cell marker, with the key for each of the cell type markers shown below. In many cases, glioblastoma cancer stem cell markers co-express within a tumor with a variety of cell type markers.

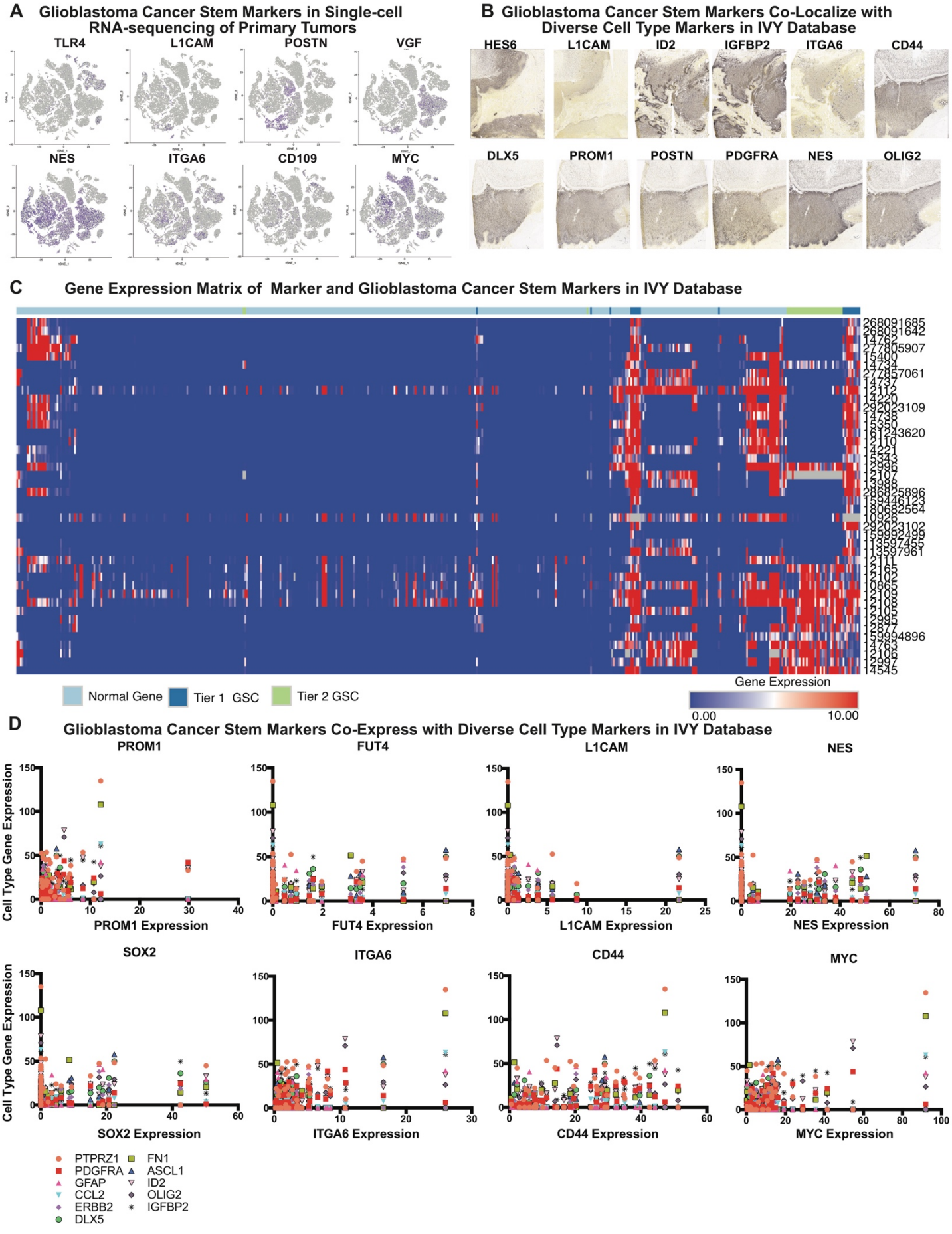
A
Glioblastoma Cancer Stem Markers in Single-cell RNA-sequencing of Primary Tumors
TLR4
L1CAM
POSTN
VGF
NES
ITGA6
CD109
MYC
B
Glioblastoma Cancer Stem Markers Co-Localize with Diverse Cell Type Markers in IVY Database
HES6
L1CAM
ID2
IGFBP2
ITGA6
CD44
DLX5
PROM1
POSTN
PDGFRA
NES
OLIG2
C
Gene Expression Matrix of Marker and Glioblastoma Cancer Stem Markers in IVY Database
Normal Gene
Tier 1 GSC
Tier 2 GSC
Gene Expression
0.00
10.00
D
Glioblastoma Cancer Stem Markers Co-Express with Diverse Cell Type Markers in IVY Database
PROM1
FUT4
L1CAM
NES
SOX2
ITGA6
CD44
MYC
Cell Type Gene Expression
PROM1 Expression
FUT4 Expression
L1CAM Expression
NES Expression
SOX2 Expression
ITGA6 Expression
CD44 Expression
MYC Expression
PTPRZ1
PDGFRA
GFAP
CCL2
ERBB2
DLX5
FN1
ASCL1
ID2
OLIG2
IGFBP2

Supplemental Figure 4 (Related to Figure 3). Using single cell RNA-sequencing to identify tumor and normal cells within the dataset a) Distribution of copy number by chromosome is observed for each sample. Graph of this distribution as well as the summary bar charts and dot plots used to determine normal vs tumor cell identity is depicted. **b)** Binned distribution per chromosome depicts the amplification (red) or deletion (blue) as detected from binned analyses from the transcriptome analysis (top) or from the exome sequencing (bottom). These plots show substantial correspondence between the analyses, validating the efficacy of the approach in the 10X data. **c)** Empirical FDR is calculated via permutation analysis, and shows an FDR of 0.002. **d)** Validation of the CNV analysis from transcriptome as compared to exome analysis shows that > 95% of CNV calls are concordant between analyses, showing the transcriptional analysis is an appropriate way of identifying CNVs and normal cell annotations. **e)** Cell type composition of cells annotated as tumor or normal, averaged across all five tumors analyzed with CNV analysis. Normal cells are more enriched for microglia, macrophages and oligodendroctyes while normal cells are enriched for oligodendrocyte precursor cells (OPCs) and radial glia.

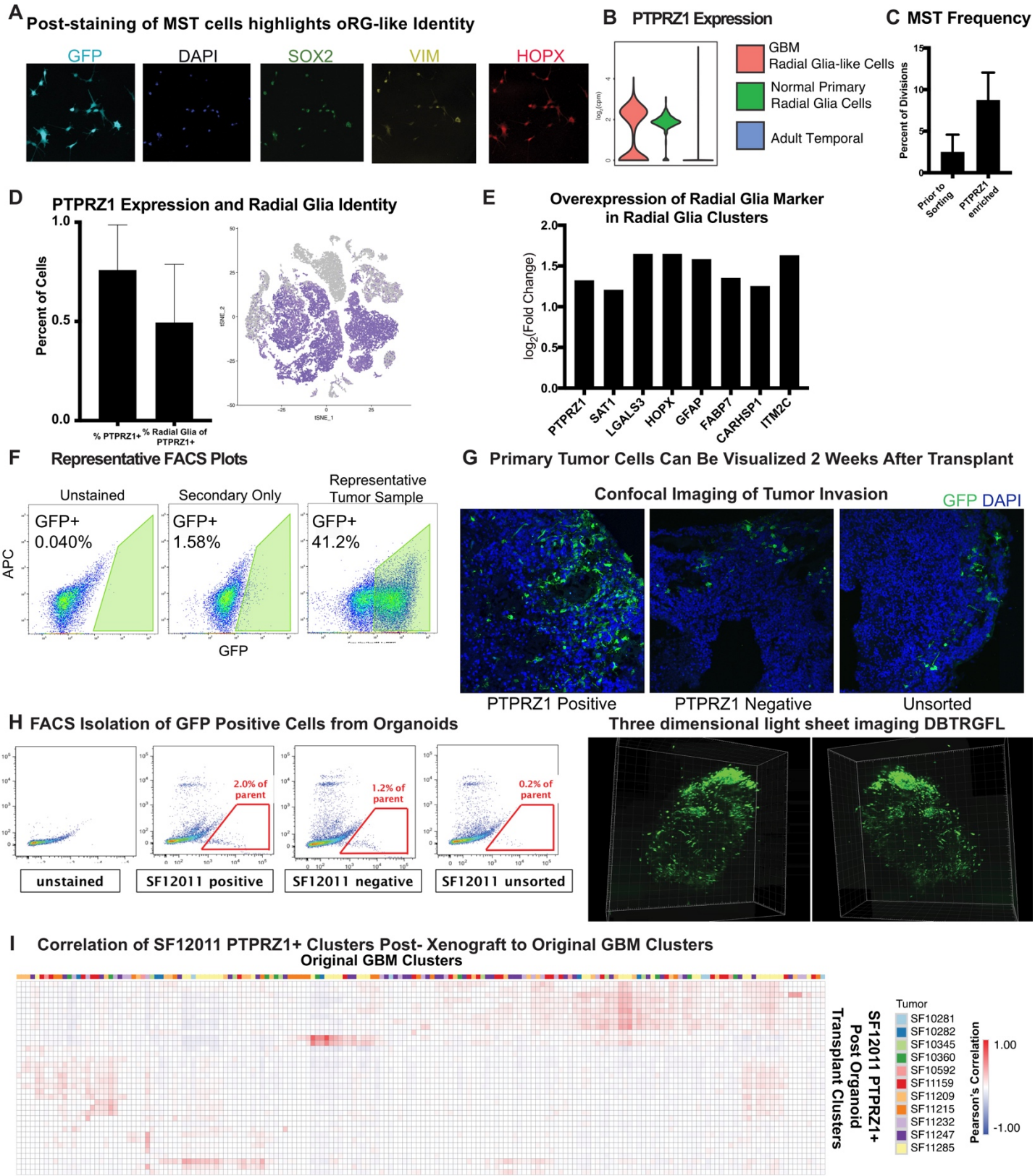

Supplemental Figure 5 (Related to Figure 5). Enrichment of PTPRZ1 positive cells a) Staining of dissociated GBM cells after MST events identifies expression of progenitor markers that are enriched in outer radial glia cells: SOX2, VIM and HOPX. **b)** Violin plot shows expression of PTPRZ1 in GBM developmental radial glia-like cells, primary developmental radial glia and adult temporal lobe samples. **c)** Graph showing the proportion of MST-like division in unsorted and enriched PTPRZ1-positive samples. **d)** Graph depicts the percent of cells that are PTPRZ1-positive and the percent of designated radial glia-like cells that are PTPRZ1-positive. Mean and standard deviation across 11 sequenced tumors shown. On the right, a feature plot

depicting PTPRZ1 expression across the 11 tumors is presented. **e)** Fold-change enrichment of outer radial glia genes in the radial glia cell clusters compared to remaining clusters (log_2 value shown). **f)** Representative FACS plots showing the enrichment of PTPRZ1+ cells from resected tumor specimens. **g)** On the left, still images of a movie (Video 7) of light sheet imaging of a cleared organoid 2 weeks after transplant with DBTRGFL unsorted cells that are GFP labeled. On the right, confocal images of cortical organoids being invaded by primary tumor cells from PTPRZ1+, PTPRZ1- and unsorted tumor samples. **h)** Representative FACS plots are shown for the retrieval of GFP positive cells 2 weeks after organoid transplantion. GFP positive cells were used for single-cell RNA sequencing. **i)** Correlation of SF12011 clusters from PTPRZ1-positive post-transplant experiment to each of the original GBM clusters. There is strong correspondence and also heterogeneity that reflects the initial tumoral heterogeneity.

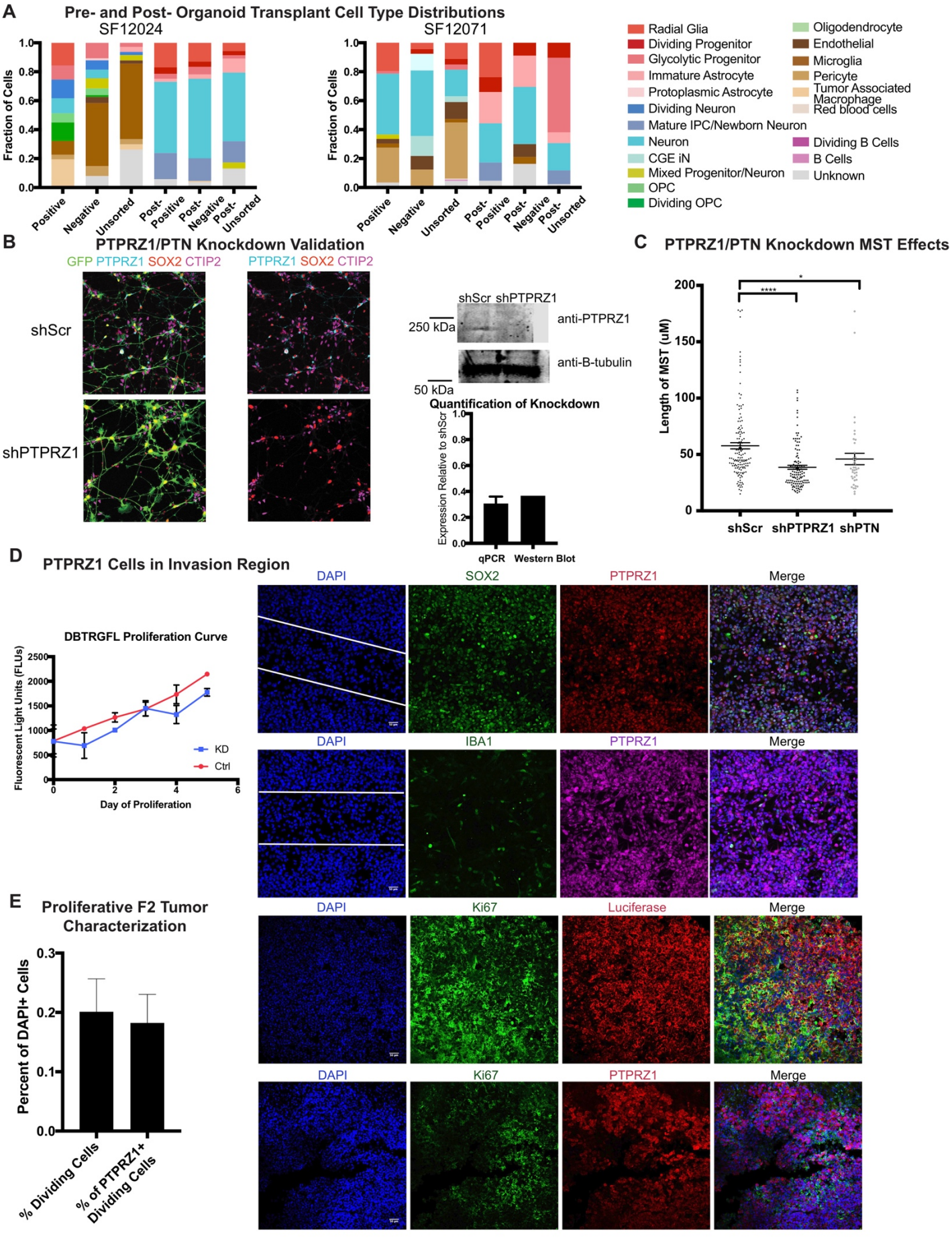
A
Pre- and Post- Organoid Transplant Cell Type Distributions
SF12024
SF12071
Fraction of Cells
Positive
Negative
Unsorted
Post-Positive
Post-Negative
Post-Unsorted
Radial Glia
Dividing Progenitor
Glycolytic Progenitor
Immature Astrocyte
Protoplasmic Astrocyte
Dividing Neuron
Mature IPC/Newborn Neuron
Neuron
CGE iN
Mixed Progenitor/Neuron
OPC
Dividing OPC
Oligodendrocyte
Endothelial
Microglia
Pericyte
Tumor Associated Macrophage
Red blood cells
Dividing B Cells
B Cells
Unknown
B
PTPRZ1/PTN Knockdown Validation
GFP PTPRZ1 SOX2 CTIP2
PTPRZ1 SOX2 CTIP2
shScr
shPTPRZ1
shScr shPTPRZ1
250 kDa
anti-PTPRZ1
anti-B-tubulin
50 kDa
Quantification of Knockdown
Expression Relative to shScr
qPCR
Western Blot
C
PTPRZ1/PTN Knockdown MST Effects
Length of MST (uM)
shScr
shPTPRZ1
shPTN
D
PTPRZ1 Cells in Invasion Region
DBTRGFL Proliferation Curve
Fluorescent Light Units (FLUs)
Day of Proliferation
KD
Ctrl
DAPI
SOX2
PTPRZ1
Merge
IBA1
Ki67
Luciferase
E
Proliferative F2 Tumor Characterization
Percent of DAPI+ Cells
% Dividing Cells
% of PTPRZ1+ Dividing Cells

Supplemental Figure 6 (Related to Figure 6). Transplants of primary glioblastoma tumors into cortical organoids a) Two additional tumor replicates are shown pre- and post-transplantiation. In each case, a graphof the most highly correlated broad cell type for each single-cell cluster is depicted as parts of a whole. Like in SF12011 (shown in figure 4), PTPRZ1 positive cells can give rise to cell types that do not exist in the initial population, particularly astrocytes and neuronal populations. **b)** Immunofluorescence of scrambled control hairpin and short hairpin targeting PTPRZ1 validates protein knockdown. Western blot and qPCR to validate knockdown (quantified across 3 replicates for qPCR) were also performed. **c)** Short hairpin induced knockdown of PTPRZ1 and its ligand PTN significantly (PTPRZ1 **** = $p < 0.0001$, PTN * = $p < 0.05$, Student's two-sided t-test) decrease the length of somal translocation length using 3 biological replicates and 4 technical replicates each in primary slice culture. **d)** Proliferation as indicated by cell titer blue assay is shown for PTPRZ1 shScr (Ctrl) or shPTPRZ1 (KD). The difference is not significant at any time point, n=5. On the right, an invasion well with white lines added to mark the bounds of the invasion chamber. Immunofluorescence shows the higher percentage of cells that are PTRPZ1 positive compared to IBA1. **e)** Immunofluorescence marking proliferating tumor cells (Ki67 for proliferation, Luciferase for tumor cells) in the DBTRGFL F2 tumor sample. PTPRZ1 positive proliferating cells are also stained and quantification using Imaris is shown in the graph on the left.